Experimental investigation and validation of neutral beam current drive for ITER through ITPA Joint Experiments

T. Suzuki [1], R. J. Akers [2], D. A. Gates [3], S. Günter [4], W. W. Heidbrink [5], J. Hobirk [4], T. C. Luce [6], M. Murakami [7], J. M. Park [7], M. Turnyanskiy [2] and the ITPA "Integrated Operation Scenarios" group members and experts

[1] Japan Atomic Energy Agency, 801-1, Mukoyama, Naka, Ibaraki-ken 311-0193, Japan
[2] CCFE/EURATOM Fusion Association, Culham Science Centre, Abingdon, UK
[3] Princeton Plasma Physics Laboratory, Princeton, NJ 08543, USA
[4] Max-Planck-Institut für Plasmaphysik, EURATOM Association, 85748 Garching, Germany
[5] University of California, Irvine, CA 92697, USA
[6] General Atomics, PO Box 85608, San Diego, CA 92186-5608, USA
[7] Oak Ridge National Laboratory, PO Box 2008, Oak Ridge, TN 37831, USA

E-mail: suzuki.takahiro@jaea.go.jp

Abstract. Joint experiments investigating the off-axis neutral beam current drive (NBCD) capability to be utilized for advanced operation scenario development in ITER were conducted in 4 tokamaks (ASDEX Upgrade (AUG), DIII-D, JT-60U, and MAST) through the international tokamak physics activity (ITPA). The following results were obtained in the joint experiments, where the toroidal field, B_t, covered 0.4-3.7 T, the plasma current, I_p, 0.5-1.2 MA, and the beam energy, E_b, 65-350 keV. A current profile broadened by off-axis NBCD was observed in MAST. In DIII-D and JT-60U, NB driven current profile has been evaluated using motional Stark effect diagnostics and good agreement between the measured and calculated NB driven current profile was observed. In AUG (at low δ~0.2) and DIII-D, introduction of a fast-ion diffusion coefficient of D_b~0.3-0.5 m^2/s in the calculation gave better agreement at high heating power (5 MW and 7.2 MW, respectively), suggesting anomalous transport of fast-ions by turbulence. It was found through these ITPA joint experiments that NBCD related physics quantities reasonably agree with calculations (with D_b=0-0.5 m^2/s) in all devices when there is no MHD activity except ELMs. Proximity of measured off-axis beam driven current to the corresponding calculation with D_b=0 has been discussed for ITER in terms of a theoretically predicted scaling of fast-ion diffusion that depends on E_b/T_e for electrostatic turbulence or β_t for electromagnetic turbulence.

PACS numbers: 52.55.Fa, 52.55.Wq, 52.35.Ra

1. Introduction and Background of NBCD Validation Efforts

NBCD is the main current drive source in ITER. In order to reach a steady-state operation scenario free from low m & n MHD activity (e.g. neo-classical tearing mode (NTM) etc.) that is resonant on low q rational surfaces, it is expected that q_{min} > ~1.5. Off-axis current drive is essential to sustain such weak or reversed magnetic shear. The negative ion-source based NB (N-NB) injector has been designed with off-axis steering capability in ITER, and the characteristics of off-axis NBCD are of great concern to achieve a Q=5 steady-state operation scenario in ITER. Concerning on-axis NBCD, the measured NBCD profile at E_b up to 370 keV using an ITER-relevant N-NB system in JT-60U showed good agreement with calculations [1,2]. Recent NSTX experiment also confirmed the good agreement for on-axis NBCD into MHD-free plasma [3]. However, there had been no result on off-axis NBCD profile, which is more important for current profile control in the steady-state operation scenario. AUG first reported off-axis NBCD from the viewpoint of current profile tailoring, where the measured off-axis NBCD current did not agree with calculations and was smaller than the calculation [4] in the case of strong heating into a low δ plasma. Later, the difference was attributed to possible diffusive redistribution of fast-ions by turbulence [5]. JT-60U also investigated the off-axis

Table 1. Operation parameters and summary of the off-axis NBCD joint experiments.

Device	AUG	DIII-D	JT-60U	MAST
I_p [MA]	0.6-0.8	0.9	1.2	0.5-0.8
B_t [T]	2-2.5	2.1	~3.7	0.4-0.5
R_p [m]	~1.65	~1.7	~3.3-3.4	~0.85
a [m]	~0.5	0.55	~0.8-0.9	~0.65
triangularity δ (ave.)	0.2-0.42	0.58	0.25-0.45	~0.35
E_b [keV]	93	81	85, 350(N-NB)	65
r/a of off-axis NBCD peak in calculation	~0.55	~0.5	~0.3(N-NB)-0.5	~0.5
the way of realizing off-axis NBCD	up/downward-steered off-axis beams	up/down-shift of the plasma	downward-steered off-axis beams	up/down-shift of plasma
codes for comparison	TRANSP	NUBEAM,TRANSP	OFMC	TRANSP
summary of results	agreement (but D_b=0.5 m^2/s at low δ=0.2 and 5MW heating power)	agreement in j_{BD} (but D_b=0.3 m^2/s at 7.2 MW heating power)	agreement in j_{BD} over wide range of E_b	broader j profile by off-axis NBCD

NBCD and found good agreement between measurement and calculation of the off-axis NBCD current, but found a difference in the NBCD location [6]. Thus, joint experiments were conducted through the ITPA to validate off-axis NBCD capability. This paper reports on the results of the joint experiments conducted in 4 tokamaks, AUG, DIII-D, JT-60U, and MAST. Since it is known that MHD activity bring about redistribution of fast-ions and modify the NBCD capability, these joint experiments were conducted in plasmas without MHD activity (e.g. sawteeth, fishbones, NTMs, Alfvén eigenmodes) except ELMs.

2. Experimental Conditions of Off-axis NBCD

Operation parameters of the devices for off-axis NBCD (as well as on-axis NBCD for comparison) are shown in table 1. Beam ions are deuterium in all discharges shown here for all devices. Positive-ion based NB's (E_b<100 keV) are used in all devices, as well as N-NB (E_b~350 keV) in JT-60U. Plasma size, shape and magnetic field vary, and the way off-axis NB injection is realized varies from device to device; use of off-axis steered NBs in AUG (up/downward) and JT-60U (downward), and vertical shift of the plasma in DIII-D (up/downward) and MAST (downward). Figure 1 shows the beam lines for off-axis NBCD in all devices and their relative position to the plasma. Locations of off-axis NBCD using positive-ion based NB (P-NB) are intended to be about a half minor radius (r/a~0.5) in all devices. In addition, off-axis NBCD at r/a~0.3 was performed in JT-60U N-NB case, which is closer to the off-axis steering NBCD in ITER. Since half of the N-NB (lower ion source injected upward) is almost on-axis (figure 1 (c)), only the other half (upper ion source injected

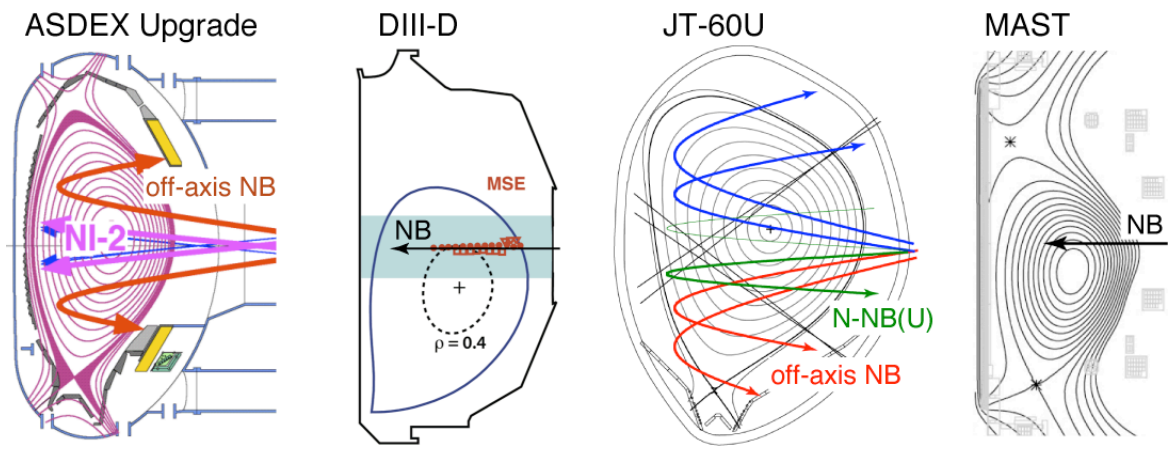

Figure 1. Beam lines for off-axis NBCD in 4 devices and their position with respect to plasma. AUG and JT-60U have exclusive off-axis beam lines, while DIII-D and MAST realized off-axis NBCD by vertical shift of the plasma.

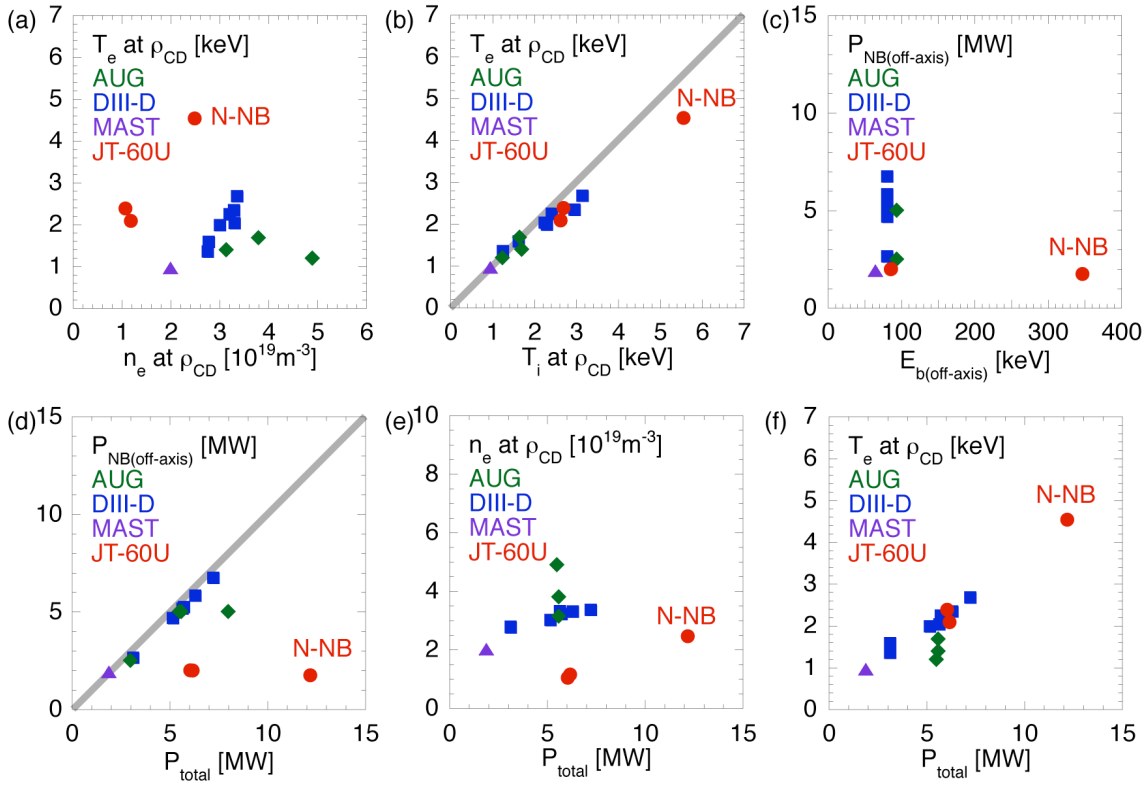

Figure 2. (a), (b) Operation regime of off-axis NBCD experiments over electron density and ion/electron temperatures at the NBCD location ρ_{CD} defined as the peak location of the beam driven current density in each calculation. In this paper, symbol shapes and colors indicate devices (AUG: green diamonds, DIII-D: blue squares, MAST: violet triangles, JT-60U: red circles). (c) Relation between off-axis NBCD power and the off-axis beam energy E_b. (d) Relation between off-axis NBCD power and total heating power P_{total}. Gray line in (d) indicates that all heating power comes from the off-axis NBCD power. (e) Electron density and (f) electron temperature as a function of P_{total}.

downward) was used for this study. MHD activity that redistributes fast-ions is avoided during NBCD analysis by adjusting operation scenarios, for example, high q_{95} operation (up to ~6) and/or pre-heating during current ramp-up to delay current penetration. In all devices, the NB driven current or change in the current profile by NB driven current is measured directly using motional Stark effect (MSE) diagnostics. The measured results are compared with theoretical calculations that are different between devices as shown in table I. There was a detailed benchmarking study between some NBCD codes using parameters of the reference ITER steady state scenario [7], where the calculated beam driven current profiles by the NUBEAM [8] (for DIII-D) and OFMC [9] (for JT-60U) codes give clear discrepancy in NB driven current (see figure 2 in reference 7). After careful investigation of the two codes, it was found that homogeneous Coulomb logarithm in the collision operator in the OFMC code is the main cause of the discrepancy in the benchmark. NB driven current by both codes agreed after revising the OFMC code. Detail of the benchmarking work is to be reported elsewhere by T. Oikawa. In this study, the above problem in the OFMC code is resolved.

3. Experimental Results

Plasma parameters (electron density n_e, electron temperature T_e and ion temperature T_i) during off-axis NBCD are summarized in figures 2 (a) and (b). The parameters are measured at the NBCD location ρ_{CD} defined as the peak location of the beam driven current density in each calculation. Figures 2 (c) and (d) show the relation of off-axis NBCD beam energy E_b, off-axis NBCD power $P_{NB(off-axis)}$ and total heating power P_{total}. Thanks to the joint experiments, wide dynamic ranges of the local plasma parameters as well as global parameters (table 1) have been achieved. Figures 2 (e) and (f) show n_e and T_e as a function of P_{total}. Roughly speaking, higher T_e was obtained at larger P_{total}. In the following, off-axis NBCD measurements in such plasmas are described in detail.

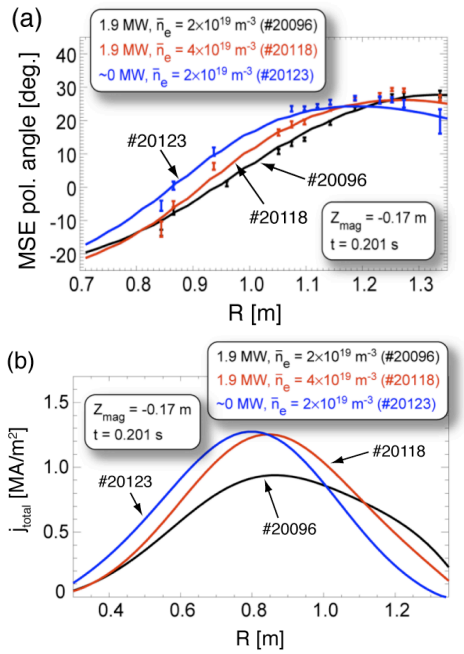

Figure 3. (a) MSE polarization angle and (b) total current density j_{total} profile measured by MSE in MAST for nearly Ohmic (#20123) and NBCD phases (#20118: higher n_e, #20096: lower n_e), showing the difference in j_{total} broadened by off-axis NBCD.

In MAST, the radial profile of the plasma current density was measured in a nearly Ohmic discharge as well as off-axis NBCD discharges [10]. A significant change in the MSE polarization angle (proportional to the magnetic field pitch angle viewed from the MSE optics) between Ohmic and off-axis NBCD discharges was observed in figure 3 (a). The resulting plasma current density profile broadened in the off-axis NBCD phase relative to the Ohmic phase at similar n_e~2x10^{19} m^{-3} as shown in figure 3 (b). In the off-axis NBCD discharge at higher n_e~4x10^{19} m^{-3}, the current density profile broadened less than at lower n_e, showing a reduction in the off-axis beam driven current with increasing n_e, qualitatively consistent with theory.

A more direct comparison of the beam driven current profile, j_{BD}, was done in DIII-D [11] and JT-60U, using loop-voltage-profile analysis [12]. Figure 4 shows the comparison between measurement and calculation in JT-60U (2.0 MW off-axis NBCD in 6.0 MW total power) and DIII-D (5.2 MW off-axis NBCD in 5.7 MW total power), as well as ITER-like slightly off-axis NBCD (ρ_{CD}~0.3) using N-NB (1.8 MW, ~350 keV) in 12 MW total power in JT-60U. The codes used for the calculations in JT-60U and DIII-D are OFMC and NUBEAM, respectively. Characteristic profile shapes and magnitudes of the beam driven current density in calculations are well validated by the measurements in figure 4. Figures 5 (a) and (b) show the comparisons of area-integrated beam driven current I_{BD} and NBCD location ρ_{CD} (peak of the beam driven current density profile j_{BD}) between measurement and calculation in DIII-D and JT-60U. AUG data plotted in figure 5 (a) as measurements are I_{BD} reproducing the measured surface loop-voltage in ASTRA code [13] under Zeff that reproduces the surface loop-voltage in on-axis NBCD phase just before the off-axis NBCD phase. This is because MSE data are not available in AUG during off-axis NBCD phase, as described later. In figure 5 (a), agreement of I_{BD} between measurements and calculations are obtained within their error bars for each machine except two DIII-D discharges with largest I_{BD}. The two discharges have the highest heating power (6.3 MW and 7.2 MW) in DIII-D data in figure 2 (d). Agreement of the NBCD

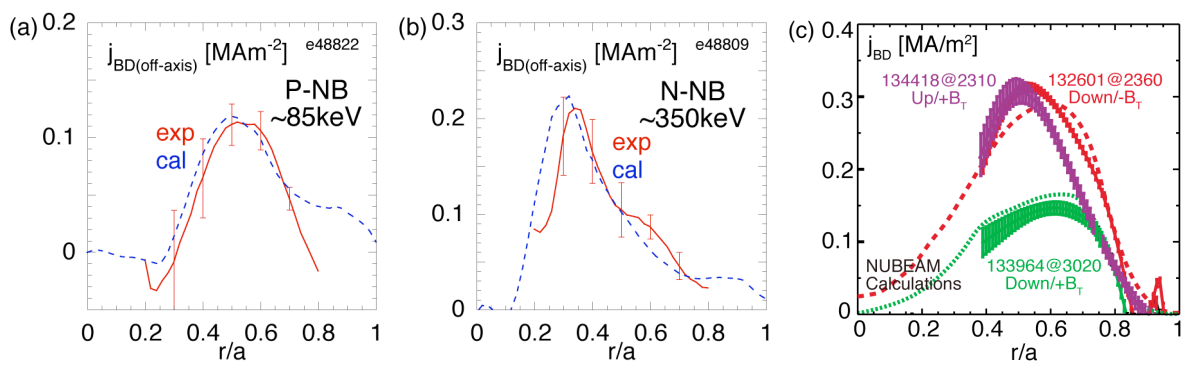

Figure 4. Comparison of the beam driven current density profile between measurement (solid curves with error bars) and calculation (broken curves). (a) JT-60U P-NB ~85 keV, (b) JT-60U N-NB ~350 keV, (c) DIII-D ~81 keV. Good agreement is observed both in JT-60U and DIII-D. In DIII-D (figure 4 (c)), NB injection angles to the magnetic field are scanned by changing the direction of the vertical shift and the direction of the toroidal magnetic field but at the same off-axis NBCD power (3 cases are shown).

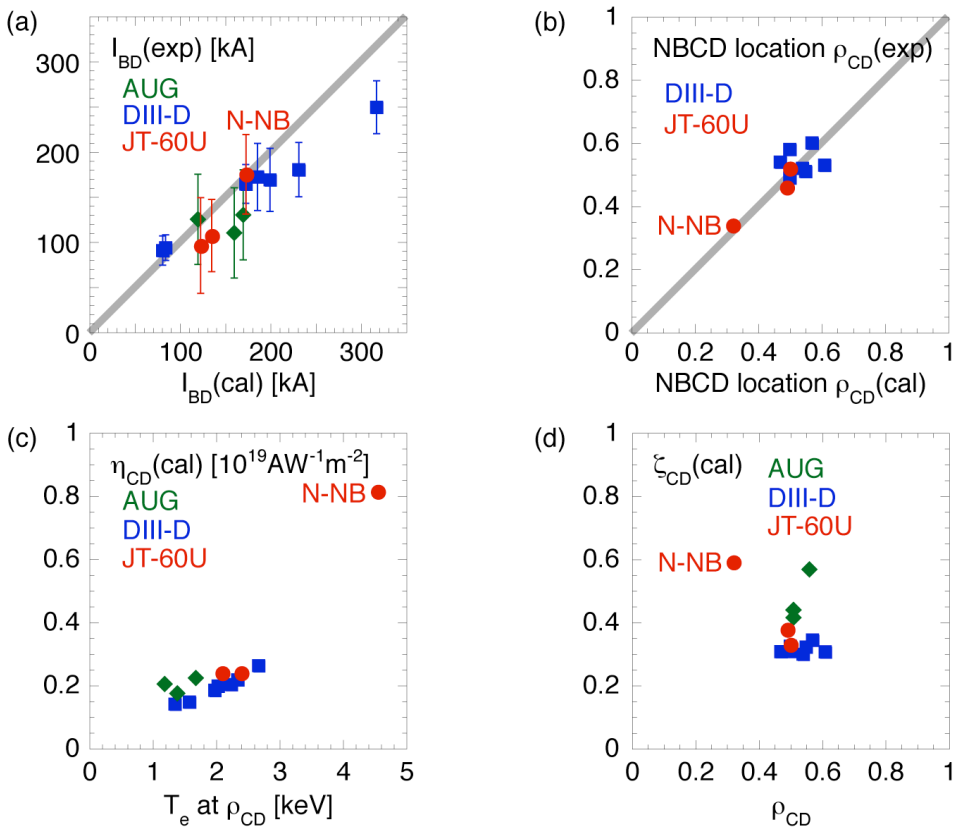

Figure 5. (a) Comparison of measured beam driven current I_{BD} and calculated one (no radial diffusion of fast-ions is taken into account) in AUG, DIII-D and JT-60U. I_{BD} for both measurements and calculations are integrated in a range r/a=0.2-0.8 in figure 4 for JT-60U. (b) Comparison of NBCD location ρ_{CD} between measurement and calculation, defined as the peak location of the beam driven current density profile. (c) Current drive efficiency as a function of T_e at NBCD location. (d) Normalized current drive efficiency as a function of NBCD location. Definition of the symbols is the same as figure 2.

location is fine for all data as shown in figure 5 (b), although it is difficult to define their error bars. Current drive efficiencies in calculations are shown in figures 5 (c) and (d) in order to show the operation regime from the viewpoint of the current drive. Dimensional current drive efficiency is defined as $\eta_{CD}=I_{BD}n_eR_p/P_{NBoff\text{-}axis}$ and normalized current drive efficiency is $\zeta_{CD}=\eta_{CD}e^3/(e_0^2k_BT_e)$, where R_p is the major radius and n_e and T_e are at ρ_{CD}. Beam driven current I_{BD} is the same as plotted in figure 5 (a).

NBCD current is theoretically predicted to depend on the NB injection angle to the magnetic field line [14,15]. In order to study the effect of NB injection angle, the direction of the toroidal magnetic field B_t, and the vertical shift of the plasma were scanned in DIII-D as shown in figure 4 (c). The measured beam driven current is almost the same between the up-shifted plasma with positive B_t (Up/+B_T) and the down-shifted plasma with negative B_t (Down/-B_T), since the NB injection angles to the magnetic field line are the same. On the contrary, a significant decrease in the beam driven current was observed in the case of off-axis NBCD in the down-shifted plasma with positive B_t (Down/-B_T). These results validate the theoretical prediction. Alignment of the NB injection angle to the magnetic field line in ITER was discussed in reference [14]. The better-alignment cases (Up/+B_T and Down/-B_T) are used as the DIII-D data in this paper for better accuracy of measurement.

In DIII-D, a discrepancy between the measured and calculated NB driven current (and profiles) was observed for the highest heating power at 7.2 MW even without MHD activity when fast-ion diffusion coefficient D_b=0 is assumed (c.f. 5.7 MW for figure 4 (c)). The measured beam driven current profile at the highest power is shown in figure 6, as well as calculations assuming various fast-ion diffusion coefficients. In this case, introducing a spatially uniform D_b=0.3 m^2/s gave better

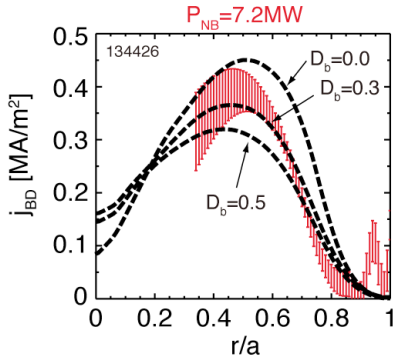

Figure 6. Comparison of the measured beam driven current density profile at 7.2 MW NBCD in DIII-D and the corresponding calculations assuming various fast-ion diffusion coefficients D_b. Best agreement to the measurement is seen in D_b=0.3 m^2/s case. The uncertainty in NBCD measurement is relatively large in the edge pedestal due to the steep variation of profiles in the edge pedestal [11]. The error bars represent random errors inferred from the variance of the time series during the stationary phase of the discharges.

agreement than D_b=0, where not only redistribution but also loss of fast-ions and resulting decrease in beam driven current are observed in the calculations with larger D_b [11]. This increased disagreement of the measured off-axis NBCD current and the corresponding calculation at higher heating power were also confirmed by other measurements of physics quantities characteristic of the fast-ion distribution function, which are the neutron emission and fast-ion D_α (FIDA) measurements [16,17].

A similar result of the dependence of off-axis NBCD on heating power had already been observed at low-triangularity, δ~0.2, in AUG [5]. Figure 7 (a) shows the comparison of the temporal evolution of the MSE polarization angle (again, proportional to the magnetic field pitch angle viewed from the MSE optics) at various minor radii between the measurement and the TRANSP [18,19] simulation. MSE data are not available during off-axis NBCD in AUG, because NTM appears when heating power increases with additional diagnostic NB for MSE. Thus, the measured MSE polarization angles are compared with the simulated ones in the decay phase after the end of off-axis NBCD in AUG. In a low-triangularity (δ=0.2) AUG discharge with 5.6 MW of heating power including 5 MW off-axis NBCD, good agreement between measurement and simulation was obtained assuming D_b=0.5 m^2/s in the simulation than D_b=0 [5]. For lower off-axis NBCD and heating powers (2.5 MW and 3 MW, respectively), the off-axis NBCD effect was as expected in ASTRA

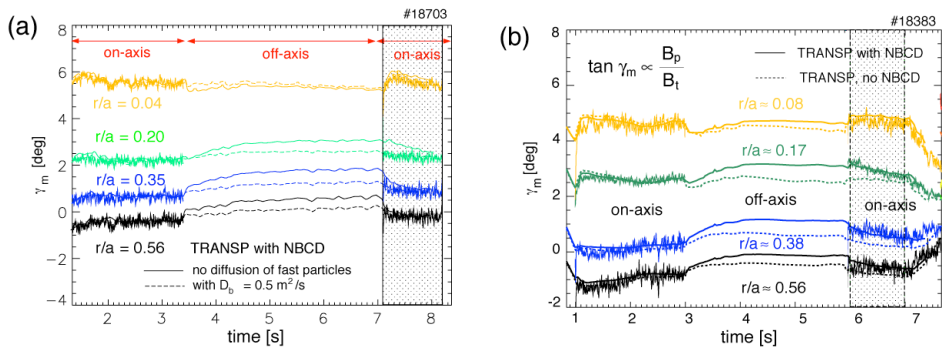

Figure 7. Waveforms of MSE polarization angles in two AUG discharges at the same off-axis NBCD and heating powers (5 MW and 5.6 MW, respectively), but different triangularities (a) 0.2 and (b) 0.4. Since MSE diagnostic data are not available during off-axis NBCD in AUG, TRANSP simulation data adjusted before the start of off-axis NBCD are compared with MSE data after the end of off-axis NBCD. In the lower triangularity discharge, MSE measurements are not properly simulated for the D_b=0 assumed (solid curves). Better agreement between measurement and simulation was obtained for D_b=0.5 m^2/s (dotted curves). (b) In another higher triangularity discharge, MSE measurement are well simulated assuming D_b=0 (solid curves). Dotted curves correspond to no NBCD effect being taken into account in the simulation.

simulations [20]. On the contrary to the low δ discharge, good agreement between MSE measurements and TRANSP simulations were observed in a higher δ=0.4 discharge (figure 7 (b)) at the same off-axis NBCD and heating powers as those in figure 7 (a). Diffusive redistribution of the fast-ions by turbulence was proposed as the cause in order to explain the observations in AUG [5].

4. Discussion

In the joint experiments described above, measurement of off-axis NBCD has been performed when there is no MHD activity except ELMs. In many cases, off-axis NBCD in a range r/a~0.3-0.5 agrees with theoretical calculations without introducing anomalous diffusion of fast-ions. In some devices and conditions (in AUG with low δ and in DIII-D), reasonably small D_b~0.3-0.5 m^2/s are required to obtain agreement between measurement and calculation at higher heating power (or off-axis NBCD power). After the work in AUG [5], there have been several theoretical works recently in the field of gyrokinetic simulation, simulating fast-ion transport induced by microturbulences [21-24]. The scalings of fast-ion diffusion coefficients based on the simulations are qualitatively similar to each other. The electrostatic diffusion of fast-ions in the background plasma with microturbulence approaches the diffusion of thermal-ions when the ratio of beam energy to the electron temperature of the background plasma (E_b/T_e) becomes smaller [21-24]. Since the thermal-ion diffusivity is, in general, larger off-axis than on-axis, the effect of microturbulence on fast-ion diffusion is significant for off-axis NBCD. In case of electromagnetic diffusion, the diffusion coefficient is independent of the beam energy and increases with plasma beta [24]. In this section, we discuss off-axis NBCD in ITER along such theoretical works, using the results in the ITPA joint experiments. It should be noted that the ITER operation scenarios have usually been developed using integrated codes with NBCD packages assuming no anomalous fast-ion diffusion. Achievement of ITER baseline scenarios within its heating and current drive capability was discussed using such integrated codes in detail in some references (e.g. references [25,26] for recent analysis). Thus, validity of the NBCD packages assuming no anomalous fast-ion diffusion under the ITER condition is important and is examined here. In the following discussions, we examine the measured beam driven current I_{BD}, not the profile j_{BD}, in comparison to the corresponding calculations, since I_{BD} well represents anomalous fast-ion diffusion at least when D_b is spatially uniform as shown in figure 6.

Figure 8 (a) shows the relation between the off-axis beam energy E_b (at injection) and T_e at the NBCD location ρ_{CD} in the joint experiments as well as one of the candidates for the ITER steady-state operation scenario (#4 Type-I) [27,28] for ρ_{CD}~0.2-0.3. The parameter E_b/T_e is estimated to be 37-40 for ITER conditions, and the results of joint experiments distribute around this value. In the joint experiments, lower E_b/T_e~37-40 near the ITER conditions are mostly obtained at higher T_e discharges with higher heating power in figure 2 (f). Figures 8 (b) and (c) plot the measured NBCD current

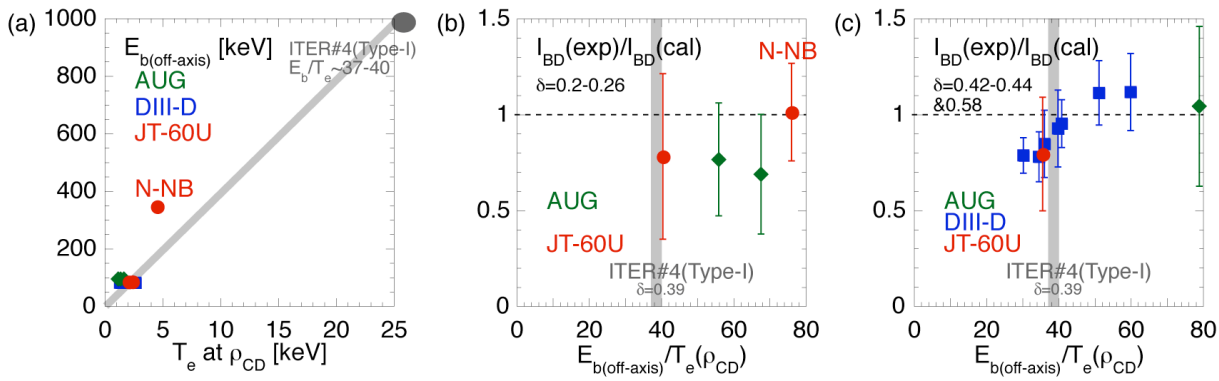

Figure 8. (a) Conditions of off-axis NBCD experiments on beam energy E_b and T_e. (b) and (c): Measured off-axis beam driven current normalized by the theoretical calculation (no radial diffusion of fast-ions is taken into account) as a function of a parameter E_b/T_e. Low-triangularity case (b), and high-triangularity case (c). The gray shaded line shows the parameter range in E_b/T_e in ITER scenario #4 (Type-I) [27,28] at δ=0.39. N-NB in JT-60U is for ρ_{CD}~0.3 and the others are for ρ_{CD}~0.5. Definition of the symbols is the same as figure 2.

normalized by the corresponding calculations for D_b=0 as a function of E_b/T_e in low and high-triangularity discharges, respectively. The low-triangularity discharge is in δ=0.20-0.26 and the high-triangularity discharge is in δ=0.42-0.44 (for AUG and JT-60U) and 0.58 (for DIII-D). Separation of discharges depending on the triangularity is based on the AUG results in figure 7. It is considered that the ratio I_{BD}(exp)/I_{BD}(cal) represents proximity to the D_b=0 condition. In high-triangularity case (figure 8 (c)), degradation of the proximity with decrease in E_b/T_e below 40 is observed, which trend is as expected from the electrostatic diffusion of fast-ions. Disagreement between measurement and calculation appears for E_b/T_e<35 in two DIII-D discharges, which is below the ITER condition. It seems the proximity is worse in low-triangularity case (figure 8 (b)) than high-triangularity case (figure 8 (c)) for ρ_{CD}~0.5 dataset. According to reference [28], the δ of the ITER scenario is 0.39, which is closer to δ in high-triangularity case than low-triangularity case. Joint experiments for off-axis NBCD at r/a~0.5 with high-triangularity (figure 8 (c)) show agreement of I_{BD} between measurement and calculation with D_b=0 around E_b/T_e~37-40 (the upper bound by DIII-D and the lower bound by DIII-D and JT-60U). The off-axis NBCD profile for JT-60U is shown in figure 4 (a) where good agreement between the measurement and the calculation was obtained. In addition, off-axis steering of ITER N-NB is intended for ρ_{CD}~0.2-0.3, so the electrostatic effect of microturbulence is relatively smaller there than for ρ_{CD}~0.5 in the joint experiments due to the smaller thermal-ion diffusion at r/a~0.2-0.3 (e.g. see figure 4 of reference 16). However, we must note that E_b/T_e in two AUG discharges shown in figures 7 are similar in a range 68-79, where the lower δ discharge (figure 7 (a)) requires D_b=0.5 m^2/s but the higher δ discharge (figure 7 (b)) requires no anomalous fast-ion diffusion. The value E_b/T_e~68 is much larger than that where DIII-D requires D_b~0.3m^2/s (E_b/T_e~30 for 7.2 MW heating case in figure 6). Thus, we must keep in mind that there could be more hidden parameters, such as geometric ones like δ.

In figure 9, data in the joint experiments are examined from electromagnetic effect of turbulence on fast-ion diffusion as well. Figure 9 (a) shows the relation between toroidal beta β_t as a measure of electromagnetic effect as a function of inverse of E_b/T_e as a measure of electrostatic effect in the database. Note that β_t and T_e/E_b (or T_e) are almost linearly coupled in DIII-D and β_t in JT-60U is restricted to low values for its high toroidal field. Figure 9 (b) and (c) show measured I_{BD} normalized by the corresponding calculations with D_b=0 assumed as a function of β_t. for low and high-triangularity discharges, respectively. No clear dependence on β_t is seen in the low-triangularity case for ρ_{CD}~0.5 data (figure 9 (b)). For high-triangularity case (figure 9 (c)), there is a degradation of the proximity with increase in β_t as predicted by theory. Disagreement appears in two DIII-D discharges for β_t>1.4%, however, this evidently comes from the correlation between β_t and T_e in DIII-D. Although there is a wide dynamic range in β_t (0.2-1.3%) for almost the same T_e/E_b=0.028

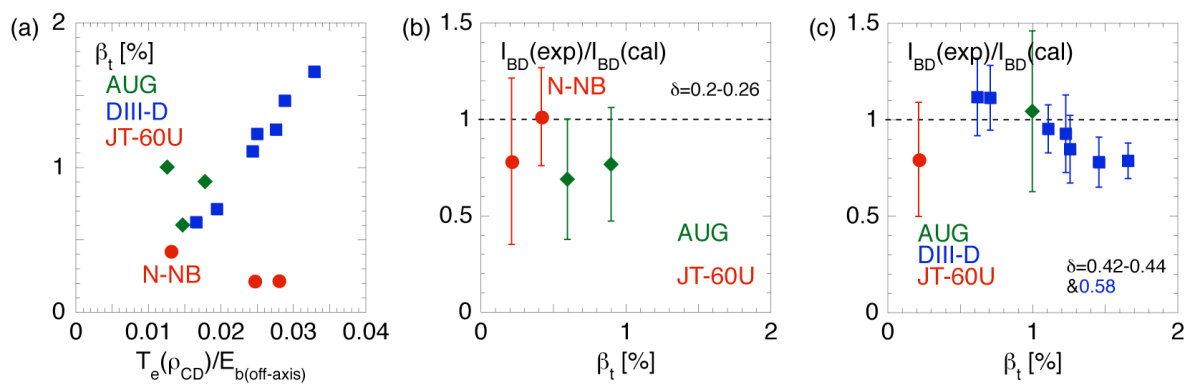

Figure 9. (a) Relation between toroidal beta β_t and inverse of E_b/T_e in the joint experiments. (b) and (c): Measured off-axis beam driven current normalized by the theoretical calculation (no radial diffusion of fast-ions is taken into account) as a function of β_t. Low-triangularity case (b), and high-triangularity case (c). Toroidal beta is ~4% in the ITER scenario #4 (Type-I) [27,28] at δ=0.39. N-NB in JT-60U is for ρ_{CD}~0.3 and the others are for ρ_{CD}~0.5. Definition of the symbols is the same as figure 2.

between DIII-D and JT-60U for high-triangularity case, it is difficult to conclude which parameters are important. In addition, in the AUG discharges with similar E_b/T_e=68-79 (or T_e/E_b=0.015-0.013), higher β_t discharge (1% at high-triangularity in figure 7 (b)) requires D_b=0, while lower one (0.6% at low-triangularity in figure 7 (a)) requires D_b=0.5 m^2/s, if difference in triangularity is ignored. Thus, it seems it is difficult to understand from the viewpoint of electromagnetic diffusion of fast-ions alone. Further theoretical understanding of fast-ion transport and/or simulation work on realistic ITER geometry and parameter is necessary. From the experimental viewpoint, separation of β_t and E_b/T_e as well as direct measurement of turbulent fluctuations (not merely a measure of turbulence E_b/T_e and β_t) are necessary for further study. It should be noted that β_t in ITER steady-state operation scenario (#4 Type-I) is about 4%, which is higher than the range in this joint experiments.

5. Summary

The following results were obtained in the ITPA joint experiments, where the toroidal field, B_t, covered 0.4-3.7 T, the plasma current, I_p, 0.5-1.2 MA, and the beam energy, E_b, 65-350 keV. The current profile was broadened by off-axis NBCD in MAST. In DIII-D and JT-60U, the NB driven current profile has been evaluated using motional Stark effect diagnostics and good agreement between the measured and calculated NB driven current profile was observed. In AUG (at low δ~0.2) and DIII-D, introduction of a fast-ion diffusion coefficient of D_b~0.3-0.5 m^2/s in the calculation gave better agreement at high heating power (5 MW and 7.2 MW, respectively), suggesting anomalous transport of fast-ions by turbulence. It was found through these ITPA joint experiments that NBCD related physics quantities reasonably agree with calculations (with D_b=0-0.5 m^2/s) in all devices when there is no MHD activity except ELMs. Proximity of measured off-axis beam driven current to the calculation with D_b=0 has been discussed for ITER in terms of a theoretically predicted scaling of fast-ion diffusion that depends on E_b/T_e or β_t. The assumption D_b=0 is usually employed in NBCD packages in integrated codes for ITER operation scenarios development so that the validity of the assumption is essential particularly for achievement of ITER steady-state operation. In the high-triangularity case with δ=0.42-0.58, degradation of the proximity has been observed for E_b/T_e<35 and β_t>1.4% in DIII-D discharges, however both of the parameters are coupled in DIII-D and identification of essential parameter for the possible turbulent transport is not possible in this joint experiment. In addition, the fast-ion diffusion coefficient required to obtain a match between the measurements and calculations in AUG differs depending on δ even at similar E_b/T_e. Thus, we must keep in mind that there could be more hidden parameters, like δ. Further theoretical understanding of fast-ion transport and/or simulation work on realistic ITER geometry is necessary. From the experimental viewpoint, separation of β_t and E_b/T_e as well as direct measurement of turbulent fluctuations (not merely a measure of turbulence E_b/T_e and β_t) are necessary for further study. The range of E_b/T_e in the joint experiment is sufficient but β_t is not for ITER steady-state operation scenario (#4 Type-I) with E_b/T_e=37-40 at ρ_{CD}~0.2-0.3 and β_t~4%. The database obtained in the ITPA joint experiments here will provide such future work with a good touchstone of benchmarking with experimental measurements.

Acknowledgments
One of the authors (TS) thanks Dr. T. Oikawa, Dr. T. Fujita, Dr. K. Hamamatsu, Dr. K. Shinohara, Dr. M. Honda and Mr. M. Suzuki for their support in improving NBCD codes (OFMC and ACCOME). Also TS thanks Dr. J. Snipes for his cooperation in improving this manuscript.

References
[1] Oikawa T. *et al* 2000 *Nucl. Fusion* **40** 435
[2] Oikawa T. *et al* 2001 *Nucl. Fusion* **41** 1575
[3] Gerhardt S. P. *et al* 2011 *Nucl. Fusion* **51** 033004.
[4] Hobirk J. *et al* 2003 *Proc. 30th EPS Conf. on Controlled Fusion and Plasma Physics (St. Petersburg)* vol 27A (ECA) O-4.1B and http://epsppd.epfl.ch/StPetersburg/start.html
[5] Günter S. *et al* 2007 *Nucl. Fusion* **47** 920

[6] Suzuki T. *et al* 2008 *Nucl. Fusion* **48** 045002
[7] Oikawa T. *et al* 2008 *Proc. 22nd Int. Conf. on Fusion Energy 2008 (Geneva, Suisse, 2008)* (Vienna: IAEA) CD-ROM file IT/P6-5 and http://www-pub.iaea.org/MTCD/Meetings/fec2008pp.asp
[8] Pankin A., McCune D., Andre R., Bateman G. and Kritz A. 2004 *Comput. Phys. Commun.* **159** 157
[9] Tani K., Azumi M., Kishimoto H. and Tamura S. 1981 *J. Phys. Soc. Jpn.* **50** 1726
[10] Turnyanskiy M., Keeling D.L., Akers R. J., Cunningham G., Conway N. J., Meyer H., Michael C. A. and Pinches S. D. 2009 *Nucl. Fusion* **49** 065002
[11] Park J. M. *et al* 2009 *Phys. Plasmas* **16** 092508
[12] Forest C. B., Kupfer K., Luce T. C., Politzer P. A., Lao L. L., Wade M. R., Whyte D. G. and Wròblewski D. 1994 *Phys. Rev. Lett.* **73** 2444
[13] Pereverzev G. and Yushmanov P. 2002 IPP-Report IPP 5/98
[14] Murakami M., Park J. M., Luce T. C., Wade M. R. and Hong R. M. 2008 *Fusion Sci. Technol.* **54** 994
[15] Murakami M. *et al* 2009 *Nucl. Fusion* **49** 065031
[16] Heidbrink W. W., Park J. M., Murakami M., Petty C. C., Holcomb C. and Van Zeeland M. A. 2009 *Phys. Rev. Lett.* **103** 175001
[17] Heidbrink W. W., Murakami M., Park J. M., Petty C. C., Van Zeeland M. A., Yu J. H. and McKee G. R. 2009 *Plasma Phys. Control. Fusion* **51** 125001
[18] Hawryluk R.J. 1980 "An Empirical Approach to Tokamak Transport," in Physics Close to Thermonuclear Conditions, edited by B. Coppi et al (Commission of the European Communities, Brussels) Vol. 1, p. 19
[19] Goldston R., McCune D., Towner H., Davis S., Hawryluk R. and Schmidt G. 1981 *J. Comp. Phys.* **43** 61
[20] Günter S., Hobirk J., Lackner K., Pereverzev G., Stabler A. and the ASDEX Upgrade Team 2004 Proc. 31st EPS Conf. on Plasma Physics (London) vol 28G (ECA) O-1.02 and http://epsppd.epfl.ch/London/start.htm
[21] Zhang W., Lin Z. and Chen L. 2008 *Phys. Rev. Lett.* **101** 095001
[22] Zhang W., Decyk V., Holod I., Xiao Y., Lin Z. and Chen L. 2010 *Phys. Plasmas* **17** 055902
[23] Hauff T. and Jenko F. 2008 *Phys. Plasmas* **15** 112307
[24] Hauff T. Pueschel M. J., Dannert T. and Jenko F. 2009 *Phys. Rev. Lett.* **102** 075004
[25] Wagner F. *et al* 2010 *Plasma Phys. Control. Fusion* **52** 124044
[26] Murakami M. *et al* 2010 Proc. 23rd Int. Conf. on Fusion Energy 2010 (Daejeon, Korea, 2010) (Vienna: IAEA) CD-ROM file ITR/P1-35 and http://www-pub.iaea.org/MTCD/Meetings/cn180_papers.asp
[27] Gormezano C. *et al.*, Progress in the ITER Physics Basis Chapter 6: Steady State Operation 2007 *Nucl. Fusion* **47** S285
[28] Polevoi A. R., Medvedev S. Yu., Pustovitov V. D., Mukhovatov V. S., Shimada M., Ivanov A. A., Poshekhonov Yu. Yu. And Chu M. S. 2002 *Proc.19th Int. Conf. on Fusion Energy 2002 (Lyon, France, 2002)* (Vienna: IAEA) CD-ROM file CT/P-08 and http://www.iaea.org/programmes/ ripc/physics/fec2002/html/fec2002.htm